Available online at www.sciencedirect.com
SCIENCE DIRECT®
Journal of Chromatography A, 1021 (2003) 61–70
JOURNAL OF CHROMATOGRAPHY A
www.elsevier.com/locate/chroma

Nuclear magnetic resonance analysis of silica gel surfaces modified with mixed, amine-containing ligands

Martha D. Bruch [a,*], Hafeez O. Fatunmbi [b]

[a] *Chemistry Department, Oswego State University, Oswego, NY 13126, USA*
[b] *Separation Methods Technologies Incorporated, Newark, DE 19711, USA*

Received 26 July 2002; received in revised form 25 August 2003; accepted 26 August 2003

Abstract

Different approaches for quantitative analysis by ^{29}Si and ^{13}C CP/MAS nuclear magnetic resonance (NMR) of silica gel chemically modified by a mixture of long and short chain amines, $-(O)_3Si(CH_2)_3N(CH_3)_2(CH_2)_{13}CH_3$ and $-(O)_3Si(CH_2)_3N(CH_3)_3$, are compared to elemental analysis. Unlike ^{29}Si NMR, variable contact time data are necessary for accurate quantitative analysis by ^{13}C NMR. Surprisingly, spectral overlap does not interfere with this approach. Surfaces prepared from reaction mixtures that consisted of 67 and 33% (v/v) long chain are found to actually contain 37 and 16% long chain amines, respectively. The mixed phase surfaces have more extensive cross-linking and fewer unreacted hydroxyls than single phase surfaces.

Keywords: Cross polarization–magic-angle spinning; Nuclear magnetic resonance spectroscopy; Stationary phases, LC; Cross-linking; Amine ligands; Silica

1. Introduction

Chemically modified silica gels are widely used as the stationary phase in high pressure liquid chromatography (HPLC), and the separation properties of these materials are strongly dependent on the structure and density of the attached ligands. Small variations in the structural details of the surface can dramatically alter both the performance and stability of HPLC columns containing modified silica gel [1–3]. Solid state nuclear magnetic resonance (NMR), using a combination of cross polarization and magic angle spinning (CP/MAS), is a well established technique for structural analysis of silica surfaces since the observed chemical shifts in a CP/MAS NMR spectrum are highly sensitive to small variations in chemical structure [1–8]; an excellent review of solid-state NMR techniques useful in the characterization of alkyl-bonded HPLC stationary phases has recently appeared [9]. The structural sensitivity of solid-state NMR is particularly important for characterization of mixed phase surfaces, in which two different ligands are reacted together to form a self assembled monolayer (SAM) that is a cross-linked mixture of the two ligands. Mixed phase surfaces have been shown to have higher densities and more extensive cross-linking than single phase surfaces prepared using the same methodology [1,10]. Consequently, mixed phase surfaces offer some advantages in terms of stability and resolution for certain types of separations [1,10–13], and it is important to be able to characterize the structural details of these mixed phase surfaces. However, mixed phase surfaces present unique analytical challenges compared to single phase surfaces. Although measurement of the extent of cross-linking on these surfaces is straightforward using ^{29}Si NMR, determination of the number and distribution of each type of chain on the surface is complicated by spectral overlap in the ^{13}C NMR spectrum of mixed phase surfaces. These are important factors when evaluating a surface for potential use as a chromatographic stationary phase. Previous work on single phase surfaces consisting of long chain alkanes of varying length indicates that both the structure and the mobility of the chains on the surface has an effect on the resolution in certain types of separations [14–17]. When the mixed phase surfaces involve chains of different lengths, variation in the number and/or distribution of long versus short chains can effect both the structure and mobility on the surface, and this most likely will effect the molecular selectivity in a chromatographic application. Consequently, intelligent

* Corresponding author. Fax: +1-3153125424.
E-mail address: bruch@oswego.edu (M.D. Bruch).

0021-9673/$ – see front matter © 2003 Elsevier B.V. All rights reserved.
doi:10.1016/j.chroma.2003.08.093

design of mixed phase surfaces to achieve better properties for specific separations necessitates quantitative analysis of the different structures on the surface. In earlier work on C_3/C_{18} mixed phase surfaces, the ratio of long chains (C_{18}) to short chains (C_3) on the surface was estimated from ^{13}C CP/MAS NMR [1], but this estimate was based on assumptions that may not be valid for all mixed phase surfaces. It is desirable to have a general method that has been validated by comparison to external, primary analytical methods.

In this paper, we compare various methods for quantitative analysis of chemically modified silica gel with mixed tertiary amine ligands attached to the surface. Two types of amines were used: (a) long chain amines, with the structure $–(O)_3Si(CH_2)_3N(CH_3)_2$ $(CH_2)_{13}CH_3$ and (b) short chain amines, with the structure $–(O)_3Si(CH_2)_3N(CH_3)_3$. Single phase surfaces, consisting of exclusively long chains (sample 1) or short chains (sample 2), were prepared in addition to mixed phase samples with an initial long chain: short chain ratio of either 2:1 (sample 3) or 1:2 (sample 4) in the reaction mixture. These modified silica gels potentially have a variety of applications when used in HPLC columns, and this will be the subject of a separate study. For example, these ligands provide amino functional groups that can be used for the separation of polar compounds. Due to the surface polarity of these ligands three or more modes of separation can be achieved. In a normal phase mode, the ligands can be used to separate polar compounds, such as substituted anilines, phenols, and chlorinated pesticides; in a reversed phase mode, separation of carbohydrates in food and beverages can be achieved. Finally, separation of organic acids and anions is possible with the addition of common buffers. It is anticipated that the distribution of long chain amine groups on the mixed phase surfaces is actually controlled by the short chain amine groups, which act as spacer groups to provide better dispersion of the long chain amines. This paper addresses the validity of this model for these mixed phase surfaces.

Aside from their potential chromatographic applications, these samples are well suited for comparison of different methods of quantitative analysis for several reasons. First of all, since the ligands contain nitrogen as well as carbon, overall ligand content can be assayed by two independent elemental analysis methods which can be compared to NMR results. Secondly, since the length of the alkyl chain is dramatically different in the two derivatizing agents used, analysis of the single phase samples provides insights into the surface mobility of long versus short chains and how any differences are manifested in the NMR results. Finally, the mixed phase samples provide an opportunity to explore the effects of spectral overlap on quantitative results obtained by NMR. Our results indicate that, for ^{13}C CP/MAS NMR, it is necessary to fit intensities obtained from variable contact time spectra to Eq. (1) in order to avoid significant distortions in the relative intensities observed at any one contact time. Furthermore, analysis of the mixed phase surfaces shows that this approach gives accurate quantitative results even in the case of spectral overlap.

2. Experimental section

2.1. Sample preparation

All samples were prepared using silica with a pore size of 60 Å, particle size of 5 μm, and specific area of 500 m^2/g. The synthesis of mixed self-assembled monolayers (SAM) of alkyl ligands is well established and has been published before [1,10,11,18]. In this study, stoichiometric quantities of long chain amine with the structure (a) $–Cl_3Si(CH_2)_3N(CH_3)_2(CH_2)_{13}CH_3$ and short chain amines, with the structure (b) $–Cl_3Si(CH_2)_3N(CH_3)_3$ are mixed in various ratios and reacted with porous silica particles under anhydrous conditions, except for a monolayer of water on the silica substrate. This method contrasts with conventional polymerization, where water is deliberately added to polymerize the reagents before bonding to the silica surface [1,10,19]. In addition to high surface coverage ($\geq$7 μmol/m^2) peculiar to this technique of bonding, repeated synthesis of SAM produced very reproducible surface coverage and retention times for test solutes [11].

2.2. Elemental analysis

All samples of the SAM phases used for this study was sent to an independent laboratory (MicroAnalysis, Wilmington, DE) for an elemental carbon, hydrogen and nitrogen analysis. The results of the study are compared with those from NMR and are summarized in Tables 2 and 4.

2.3. NMR spectroscopy

All NMR spectra were obtained at a controlled temperature of 300 K on a Bruker MSL 300 NMR spectrometer (7 Tesla magnet) using a combination of cross polarization and magic angle spinning (CP/MAS) [20]. Samples were packed into 7 mm rotors and spun at speeds between 3.0 and 3.1 kHz. The mass of the sample, typically between 150 and 200 mg, was determined by difference between the full and empty rotor. For ^{13}C spectra (75.5 MHz), 4 K data points were acquired over an effective sweep width of 33.3 kHz (440 ppm), 3600 transients were accumulated per spectrum, and contact times ranging from 0.05 to 30 ms were used in variable contact time experiments. All ^{13}C spectra were referenced externally to the methyl signal in hexamethyl benzene (HMB). For ^{29}Si spectra (59.6 MHz), 4 K data points were acquired over a spectral width of 25 kHz (420 ppm) with a total of 500 transients accumulated per spectrum. Contact times varied from 0.2 to 60 ms, and ^{29}Si spectra were referenced externally to 2,2-dimethyl-2-silapentane-5-sulfonate (DSS) at 0 ppm. For both nuclei, a relaxation delay of 2 s was used, which is longer than three times the proton spin-lattice relaxation time (T_1), estimated from inversion recovery experiments. The proton 90° pulse width was 6 μs, corresponding to a spin-lock field of 42 kHz. All spectra were processed using

an exponential filter function prior to Fourier transformation, using a line broadening parameter of either 10 Hz (^{13}C) or 20 Hz (^{29}Si). The equilibrium intensity for each signal, M_0, was determined from variable contact time CP/MAS experiments. The integrated intensities from each spectrum, $M(t)$, were measured as a function of the contact time t and were fitted to Eq. (1) using a three parameter simplex method [21].

3. Results and discussion

3.1. ^{29}Si NMR

Fig. 1 shows the ^{29}Si CP/MAS spectra of surfaces prepared using a reaction mixture of (a) exclusively long chains, (b) exclusively short chains, (c) 2:1 mixture of long to short chains, and (d) 1:2 mixture of long to short chains. There are five main peaks observed, and the assignments of these signals are well known [1,2,4–6]. The upfield peaks, from −90 to −120 ppm, represent silicon atoms at sites that do not have an attached ligand. These silicons can be in three different environments: (a) silane diols, $–O_2Si(OH)_2$, (b) silanols, $–O_3Si(OH)$, and (c) siloxanes, $–O_4Si$ have chemical shifts of approximately –90 ppm (Q^2), −100 ppm (Q^3), and −120 ppm (Q^4), respectively. Although a significant number of silane diols are observed in the unreacted silica gel (spectrum not shown), the signal at −90 ppm is negligibly small in the spectra of all four modified surfaces. This indicates that there are essentially no remaining unreacted silane diols in the modified samples.

The signals in the region from −40 to −80 ppm represent silicon sites that have an attached alkyl chain. The peaks at shifts of approximately −50,−60, and −70 ppm represent sites that have two remaining hydroxyl groups ($–OSi(OH)_2R$), one hydroxyl group ($–O_2Si(OH)R$), and no hydroxyl groups ($–O_3SiR$), respectively and are designated T^1, T^2, and T^3. Quantitative analysis of these structures is complicated by the fact that the intensity of each signal in a CP/MAS spectrum depends upon the efficiency of cross polarization (T_{CP}) and the proton relaxation time ($T_{1\rho}$) in addition to the number of nuclei that give rise to that signal [20]. Hence the relative intensities will be distorted in a spectrum obtained with a single contact time if the relative values of T_{CP} and $T_{1\rho}$ are different in different structures. The most reliable approach to quantitative analysis using CP/MAS involves acquisition of a series of spectra obtained with different cross-polarization contact times. The integrated intensities, $M(t)$, from this variable contact time data can be fitted to Eq. (1) to obtain the equilibrium intensities, undistorted from difference in cross-polarization efficiency or relaxation [20,22].

$$M(t) = M_0 \left(1 - \frac{T_{CP}}{T_{1\rho}}\right)^{-1} \times \left\{\exp\left(\frac{-t}{T_{1\rho}}\right) - \exp\left(\frac{-t}{T_{CP}}\right)\right\} \quad (1)$$

However, this approach requires enormous amounts of instrument time for data acquisition (typically 2 days per sample), so an alternative approach is desirable if loss of accuracy can be avoided. Previous work on single phase surfaces indicates that the relative values of T_{CP} and $T_{1\rho}$ are invariant with structure so that reliable quantitative results can be obtained from a single ^{29}Si CP/MAS spectrum [15,23,24]. To verify this assumption for mixed phase surfaces, the relative intensities of the peaks for T^1, T^2, and T^3 structures obtained from a single spectrum were compared to the equilibrium intensities (M_0 values) obtained from fitting each peak separately to Eq. (1), and these results are summarized in Table 1. The percentages of the three types of structures obtained by the two methods are the same within experimental error. These results confirm that it is unnecessary to perform a time consuming variable contact time experiment to get

Table 1
Comparison of single and variable contact time ^{29}Si CP/MAS results

	Sample 1 long only	Sample 2 short only	Sample 3 mixed 2:1	Sample 4 mixed 1:2
T^1 5 ms[a] (%)	25	16	15	10
T^1 M_0[b] (%)	25	18	16	12
OH ^{1}H $T_{1\rho}$ for T^1 (ms)	18[c]	12	18	17
T^2 5 ms (%)	61	61	66	63
T^2 M_0 (%)	62	61	65	63
OH ^{1}H $T_{1\rho}$ for T^2 (ms)	17	14	19	19
T^3 5 ms (%)	14	23	19	27
T^3 M_0 (%)	13	21	19	25
OH ^{1}H $T_{1\rho}$ for T^3 (ms)	16	16	22	21
Cross-linking[d] (%)	67	71	70	73

[a] Obtained from a single contact time of 5 ms. Estimated absolute uncertainty is ±3%.
[b] Obtained from fitting variable contact time data to Eq. (1). Estimated absolute uncertainty is ±2%.
[c] ^{1}H $T_{1\rho}$ values for surface hydroxyls associated with each of the three structures were obtained by fitting variable contact time data to Eq. (1). Estimated uncertainty is ±2 ms. T^1: $–OSi(OH)_2R$; T^2: $–O_2Si(OH)R$; T^3: $–O_3SiR$; R: amine ligand.
[d] Obtained from Eq. (2) using variable contact time results [14].

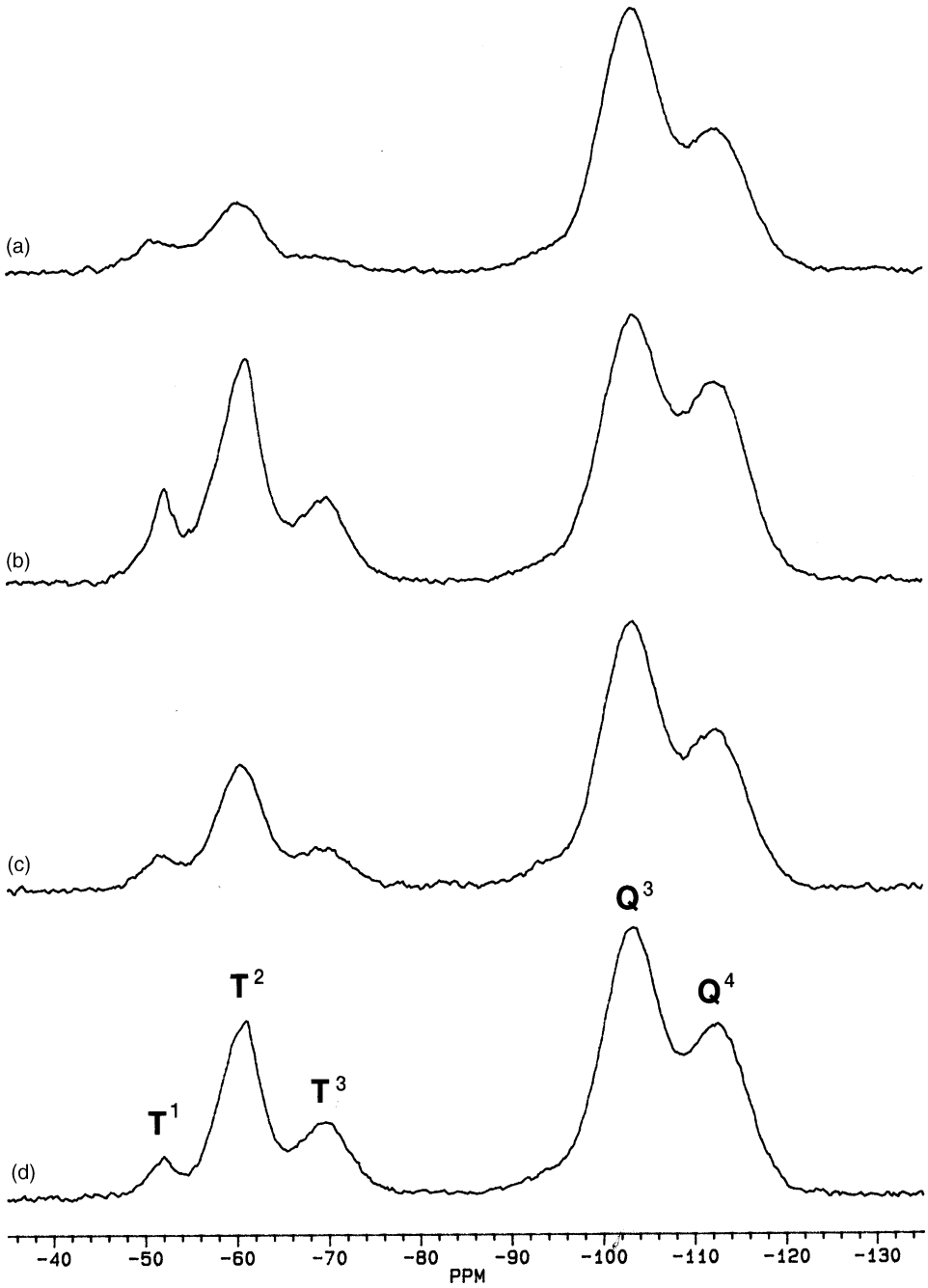

Fig. 1. ^{29}Si CP/MAS spectra (5 ms contact time) of surfaces prepared with (a) exclusively long chains, (b) exclusively short chains, (c) mixed phase with a reaction ratio of 2:1 long to short chains, and (d) mixed phase with a reaction ratio of 1:2 long to short chains.

reliable quantitative data from ^{29}Si NMR; a single contact time is sufficient. Since the maximum intensity is typically observed for a contact time between 2 and 5 ms, 5 ms is a good choice in order to optimize the signal-to-noise ratio of the spectrum in the minimal time.

External verification of the ^{29}Si NMR quantitative results can be obtained by comparing the NMR results to the percent nitrogen from elemental analysis. The sum of the equilibrium intensity of peaks due to T^1, T^2, and T^3 structures is proportional to the total number of alkyl chains attached to the surface. Since each of these structures contains exactly one nitrogen atom, this sum divided by the sample mass is proportional to the percent nitrogen determined by elemental analysis. To facilitate an easy comparison, the NMR data were normalized so that the value for sample 1, exclusively long chains, is equal to the percent nitrogen obtained from elemental analysis for that sample (0.90%), and the results are summarized in Table 2. In general, good agreement is observed between NMR and elemental anal-

Table 2
Comparison of ^{29}Si NMR results and percent nitrogen from elemental analysis

Sample	Elemental analysis % nitrogen	^{29}Si NMR		
		Total intensity ($T^1 + T^2 + T^3$)		Unreacted OH ($Q^2 + Q^3$)
		M_0[a]	5 ms[b]	M_0
1 (long chain only)	0.90	0.90[c]	0.90[c]	2.23
2 (short chain only)	2.01	2.23	2.08	1.82
3 (2:1 long:short)	1.22	1.26	1.27	2.03
4 (1:2 long:short)	1.71	1.52	1.59	1.65

[a] Variable contact time data was fitted to Eq. (1) to obtain the equilibrium intensity for each of the three peaks T^1, T^2, and T^3 separately. These intensities were summed and divided by the mass of the sample. Estimated relative uncertainty is ±10%.
[b] Intensities for T^1, T^2, and T^3 from a single contact time spectrum (5 ms) were summed and divided by the sample mass. Estimated relative uncertainty is ±10%.
[c] All NMR intensities were normalized to the value of 0.90% nitrogen obtained by elemental analysis for sample 1.

ysis results, irrespective of whether variable contact time data or intensities from a spectrum obtained with a single contact time were used.

However, since the ^{1}H $T_{1\rho}$ values for the unreacted hydroxyls are significantly longer than for the hyroxyls near sites of ligand attachment, significant distortions arise in the ratio of attached ligands to unreacted hydroxyls if Q^2 and Q^3 intesities are compared to T^1, T^2, and T^3 intensities in a ^{29}Si CP/MAS spectrum obtained with a single contact time. These observations are consistent with previous results on single phase surfaces [24]. Consequently, variable contact data were used to determine the amount of unreacted hyroxyls on the surface. The results were normalized as described in the previous paragraph to facilitate direct comparison with the number of ligands on the surface determined from variable contact time CP/MAS data and are summarized in Table 2.

Comparison of the distributions of T^1, T^2, and T^3 structures observed in the four samples reveals some interesting differences. The single phase surface consisting exclusively of short chains has a greater density of attached ligands and a smaller density of unreacted hydroxyls than the surface prepared using only long chains (Table 2), presumably because the short chains have an easier time adding to a crowded surface than do long chains due to steric considerations. Incorporation of short chains also results in more T^3 and fewer T^1 structures than in the single phase surface containing only long chains. The percentage of cross-linking can be calculated from the percentages of T^1, T^2, and T^3 structures using Eq. (2) [14].

$$\%\,\text{cross-linking} = \tfrac{1}{2}(\%T^1) + \tfrac{2}{3}(\%T^2) + \%T^3 \quad (2)$$

This calculation shows that using short chains results in more extensive cross-linking than long chains in single phase surfaces, as expected based on steric considerations. Some surprising results are obtained, however, when the mixed phase surfaces are compared to the single phase surfaces. The mixed phase with the larger amount of long chains (sample 3) has ligand density, density of unreacted hydroxyls, and percent cross-linking that is in between the two single phase surfaces. This is consistent with previous results on mixed phase surfaces [1,10] and confirms the expectation that short chains will fit in between long chains and cross-link more completely than on a single phase surface containing exclusively long chains. By contrast, a single phase surface with only short chains is expected to have a greater ligand density and more extensive cross-linking than the mixed phase surface due to the greater reactivity and smaller size of the short chains, and this observed for sample 3. However, different behavior is observed when the ratio of long to short chains is reduced (sample 4). Although the ligand density of this mixed phase surface is lower, as expected, than for the single phase surface with short chains, the density of unreacted hydroxyls is actually *lower* on the mixed phase surface (Table 2). Furthermore, this mixed phase surface is more extensively cross-linked than the short-chain single phase surface, with the mixed phase containing a higher percentage of T^3 structures at the expense of T^1 structures (Table 1). The cause of this unexpected result is not known, but the presence of a small number of long chains on a crowded surface may exert an influence on the chain conformation that enables the short chains to pack together more effectively to produce greater cross-linking on the surface. Whatever the cause, this effect disappears when a greater number of long chains are incorporated. These results suggest there is an optimum ratio of long to short chains that will maximize cross-linking and minimize unreacted hydroxyls on mixed phase surfaces. Since resistance to degradation from processes like hydrolysis is improved by minimizing surface hydroxyls and maximizing cross-linking, mixed phase surfaces incorporating the optimal ratio of long and short chain amines should offer increased stability over either single phase surface.

Further insights can be gained by examining the ^{1}H $T_{1\rho}$ values for the hydroxyl groups obtained by fitting variable contact time data to Eq. (1) (Table 1). The hydroxyl relaxation times are similar regardless of the type of structure, and are similar to those observed previously for both C_{18} single phase and C_3/C_{18} mixed phase surface hydroxyls [1].

These results suggest that spin diffusion among the hydroxyl protons is efficient and that the mobilities of the surface hydroxyl protons are largely unaffected by either the length or the nature of the attached ligand. However, the ^{1}H $T_{1\rho}$ values for the single phase surface containing only short chains are somewhat shorter than those for either of the mixed phase surfaces, which suggests the hydroxyls on the mixed phase surfaces are more mobile than on the single phase surface. Increased flexibility could make it easier for ligands to add to a crowded surface, so this may facilitate greater cross-linking. Hence, the unexpected result discussed above for mixed phase sample 4 may be due, at least partially, to dynamic effects on the surface.

3.2. ^{13}C NMR

^{29}Si NMR is an excellent probe of the nature of the silicon sites where ligands are attached in chemically modified silica. To learn anything about the nature of the attached ligands themselves, however, it is necessary to invoke ^{13}C NMR. In particular, under the right conditions for obtaining reliable intensities, ^{13}C NMR can be used, in principal, to obtain the relative amount of two different ligands on the surface of a mixed phase sample. Before the mixed phase sample can be analyzed, it is necessary to determine under what conditions quantitative results can be obtained, using the single phase samples as controls.

^{13}C CP/MAS spectra of the single and mixed phase surfaces are shown in Fig. 2. Assignment of the resonances can be done based on chemical shifts and comparison to previously assigned ^{13}C spectra of modified surfaces [5,6]. The spectrum of the surface with only short chain ligands (Fig. 2b) has three resonances at 12, 20, and 70 ppm corresponding to the three methylene carbons in the α, β, and γ positions, respectively relative to the silicon atom, and the three equivalent methyl carbons give rise to a large, sharp signal at 54 ppm. Since partial overlap of the signals at 12 and 20 ppm make it difficult to obtain accurate, separate integrals for these two peaks, these two peaks were integrated together. Consequently, the expected intensity ratio is 1:3:2 for the peaks at 70 and 54 ppm, and the sum of the peaks at 12 and 20 ppm, respectively. Relative intensities obtained from a spectrum at a single contact time and from fitting variable contact time spectra to Eq. (1) are summarized in Table 3. For the equilibrium intensities obtained from variable contact time data, there is excellent agreement between the observed and expected intensities. However, significant distortions in the relative intensities are observed when any one contact time is used. The relative intensities of the methylene carbons in an individual CP/MAS spectrum are reasonably accurate, but the intensity of the methyl is underestimated at short contact times and overestimated at long contact times. This is most likely due to a difference in molecular motion for the methyl groups at the end of the chain relative to the methylenes near the surface, as evidenced by the observation that the alkyl chain ^{1}H $T_{1\rho}$ values obtained from fitting variable contact time data are twice as long for the methyls as for the methylenes. This observation is consistent with previous results indicating that terminal methyl groups have increased mobility on single phase surfaces containing C_{18} and C_{21} alkyl chains [24–26].

Table 3
^{13}C intensities for the surface with exclusively short chains estimated from variable vs. single contact time data

Peak	M_0[a]	1 ms[b]	2 ms[b]	5 ms[b]	Theoretical[c]
70 ppm	1.00[d]	0.855	0.636	0.440	1
54 ppm	2.99	2.31	2.62	2.25	3
12 and 20 ppm	2.11	1.67	1.43	0.910	2

[a] Obtained by fitting variable contact time data to Eq. (1). Estimated relative uncertainty is ±10%.
[b] Obtained from a single contact time spectrum with the contact time indicated. Estimated relative uncertainty is ±10%.
[c] Theoretical relative intensities expected based on the number of carbon nuclei associated with each signal in the ^{13}C CP/MAS spectrum.
[d] All values were normalized to a value of 1.00 for the intensity of the peak at 70 ppm obtained from fitting variable contact time data to Eq. (1).

The ^{13}C spectrum of the surface containing exclusively long chains (Fig. 2a) is more complicated than that for short chains. Due to spectral overlap, two or more distinctly different structures contribute to the intensity of each region in the spectrum. If the overlap is among signals arising from structures with different mobility, e.g. carbons at different positions in the chain, the relaxation times for the overlapping signals may be different. Indeed, previous work indicates that, unlike the case of the surface hydroxyls, spin diffusion is not efficient among the protons in the ligands attached to the surface [15,27], and variations in the ^{1}H $T_{1\rho}$ values are expected. In this case, fitting the variable contact time data to Eq. (1) using a single set of parameters could possibly lead to distortions in the relative intensities obtained from this method. To see if equilibrium intensities obtained from curve fitting variable contact time data are accurate in the case of spectral overlap, three regions were integrated and fit separately: (1) the peak at 55 ppm representing three carbons (two methyls and a methylene), (2) the peak at 70 ppm representing two methylene carbons, and (3) the entire upfield region from 0 to 40 ppm, representing the remaining 14 carbons. The relative intensities obtained from curve fitting are 2.74, 2.33 and 14.0 for these three regions, respectively, which agree reasonably well with the expected ratio of 3:2:14. Although it is obvious that spectral overlap of signals due to carbons of different mobility causes some inaccuracies in the relative intensities, this method is reliable enough to get reasonable estimates (±10%) for the relative amounts of the two ligands present in the mixed phase surfaces.

The accuracy of quantitaive results obtained from ^{13}C CP/MAS spectra with the method described above can be further evaluated by comparing the total carbon content from NMR (obtained by summing all M_0 values and dividing by the sample mass) with percent carbon obtained from ele-

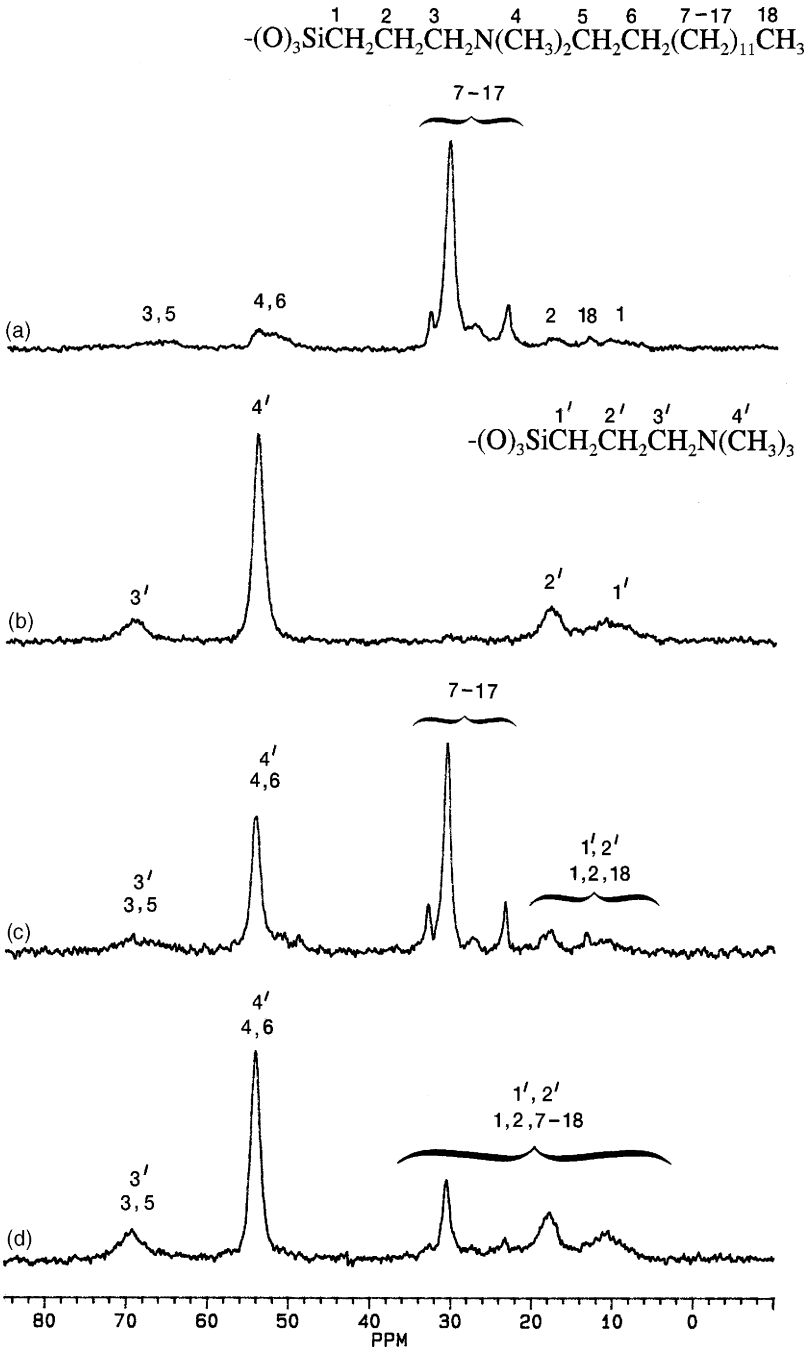

Fig. 2. ^{13}C CP/MAS spectra (2 ms contact time) of surfaces prepared with (a) exclusively long chains, (b) exclusively short chains, (c) mixed phase with a reaction ratio of 2:1 long to short chains, and (d) mixed phase with a reaction ratio of 1:2 long to short chains.

mental analysis. The total carbon content from NMR was normalized to the percent carbon obtained from elemental analysis for the sample consisting exclusively of long chains, and the results are summarized in Table 4. This approach, which has been shown to give reliable estimates for percent carbon in other mixed phase samples [1], also gives good results in this case, with excellent agreement between elemental analysis and NMR results for percent carbon. To determine the relative amount of long chain versus short chain ligands in the mixed phase samples, integrated intensities from variable contact time spectra for the three regions described above were fitted separately to obtain equilibrium intensities (M_0 values) for these three regions. Since both the long and short chains contribute three carbons apiece to the peak at 55 ppm, dividing this intensity by three gives a measure of the sum of the number of long chains (A) and short chains (B). Similarly, the upfield region contains two carbons for each short chain and fourteen carbons for each long chain. Hence, two Eqs. (3) and (4), can be written for the number of long and short chains, and these two equa-

Table 4
Comparison of percentages of carbon and nitrogen estimated from ^{13}C NMR vs. elemental analysis

Sample	Percent carbon		Percent nitrogen	
	^{13}C NMR[a]	Elemental analysis	^{13}C NMR[c]	Elemental analysis
1 (long chains only)	14.3[b]	14.3	0.88	0.90
2 (short chains only)	10.2	10.7	1.98	2.01
3 (2:1 long:short)	11.2	10.8	1.21	1.22
4 (1:2 long:short)	11.4	10.9	1.65	1.71

[a] Obtained from fitting variable contact time data for each peak to Eq. (1), summing the resultant M_0 values, and dividing by the mass of the sample.
[b] NMR results are normalized to a value of 14.3 for the long chain sample.
[c] Obtained from solving Eqs. (3),(4),(6) and (7) (see text for details).

tions can be solved simultaneously for A and B.

$$\mathrm{A} + \mathrm{B} = \tfrac{1}{3}(M_0 \text{ at } 55 \text{ ppm}) \quad (3)$$

$$14\mathrm{A} + 2\mathrm{B} = M_0 \text{ for upfield region} \quad (4)$$

As a check on the validity of the solutions to Eqs. (3) and (4), the expected intensity for the peak at 70 ppm can be calculated based on these solutions and compared to the experimental value. Since the peak at 70 ppm represents two carbons for each long chain and one carbon for each short chain, the solutions to Eqs. (3) and (4) should also satisfy Eq. (5).

$$2\mathrm{A} + \mathrm{B} = M_0 \text{ at } 70 \text{ ppm} \quad (5)$$

In all cases, the calculated value for M_0 at 70 ppm agrees with the experimental value within ±10%, which indicates that solving Eqs. (3) and (4) simultaneously yields reliable estimates for the relative number of long and short chains. Using this method, mixed phase sample 3, prepared from a 2:1 mixture of long to short chains was found to actually contain only 37% long chains on the surface, while sample 4, prepared from a 1:2 mixture of long to short chains consists almost exclusively of short chains, with only 16% long chains actually on the surface.

While the approach described above only gives the ratio of long to short chains, this information can be used in combination with the percent carbon obtained by NMR to calculate the number of long (x) and short (y) chains per 100 g of sample. Since long and short chains contain 19 and 6 carbons per chain, respectively, the number of long and short chains per 100 g of sample are related to percent carbon according to Eq. (6).

$$\%\,\text{carbon} = (12)(19)x + (12)(6)y \quad (6)$$

Since the ratio of long to short chains (x/y) is known, Eq. (6) can be solved to obtain the number of both long chains (x) and short chains (y) on the surface for every 100 g of sample. Using the normalized NMR values for % carbon (Table 4), Eq. (6) yields values of 0.063 long chains and 0.142 short chains per 100 g of sample for the two single phase surfaces. The mixed phase surface which is 37% long chains has 0.032 long chains and 0.054 short chains per 100 g, whereas the mixed phase surface which is 16% long chains has 0.019 long chains and 0.099 short chains per 100 g. These results show that the total density of ligands, irrespective of type, increases as the percentage of short chains on the surface increases, and this is consistent with the greater reactivity of the short chains.

Although the ^{13}C NMR results reveal the *number* of long and short chains on the surface, this does not give information about the *distribution* of long versus short chains. Some insight can be gained by examining the mobility of the attached ligands as manifested by the alkyl proton $T_{1\rho}$ values, which is a probe of motion in the kHz range [20]. Unfortunately, spectral overlap of signals causes ambiguities in the interpretation of relaxation times for mixed phase surfaces. The most reliable probe is the peak at 55 ppm which is primarily due to the methyls attached to the nitrogen in both long and short chains. The $T_{1\rho}$ value for these methyls is significantly longer in the single phase surface consisting of short chains (12 ms) than for the surface with exclusively long chains (8 ms), and the T_{CP} values are also slightly longer for the short chains. These observations suggest decreased mobility for the methyls in long chains. Unfortunately, spectral overlap prevents measurement of separate relaxation times for the two ligands in mixed phase surfaces; only an average can be obtained. However, if the mixed phase surface consisted of blocks of long chains connected to blocks of short chains, the relaxation times for the mixed phase would be in between the two single phase values. By contrast, the measured relaxation times for the 37 and 16% mixed phase surfaces are 14 and 12 ms, respectively. These results suggest that, in both cases, the long chains tend to be surrounded by short chains so that the overall mobility of the mixed phase surfaces is comparable to that of the single phase of short chains. The slightly longer values observed for the mixed phase with 37% long chains may reflect the lower total density of ligands in the mixed phase, which probably results in a less rigid surface.

As a final check on the accuracy of the number of long and short chains obtained from ^{13}C NMR, the NMR results can be used to predict the percent nitrogen expected from elemental analysis. Since each chain of either type contains one nitrogen per chain, the percent nitrogen can be calculated from the solution to Eq. (6) using Eq. (7).

$$\%\,\text{Nitrogen} = 14(x + y) \quad (7)$$

Eqs. (6) and (7) were used to calculate the percent nitrogen for all four samples based on the ^{13}C NMR results, and the results are summarized in Table 4. There is excellent agreement between the percent nitrogen estimated from the ^{13}C NMR results and that obtained from elemental analysis. This confirms that detailed quantitative infornation about the number and type of ligands on the surface of modified silica gel can be obtained from ^{13}C CP/MAS NMR, but only if intensities from variable contact time spectra are fit to Eq. (1) to obtain equilibrium intensities, undistorted by differences in cross-polarization efficiency and/or mobility of different carbons in the chain.

4. Conclusions

^{29}Si CP/MAS NMR was used to determine the amount of different types of silicon sites present on the surface of a series of chemically modified silica gels. Quantitative results from a ^{29}Si spectrum obtained with a single contact time are indistinguishable from those obtained by fitting intensities from a series of spectra, obtained at different contact times, to get equilibrium intensities. These results indicate that, for both single and mixed phase surfaces, the time consuming process of obtaining variable contact time data is unnecessary to obtain reliable results from ^{29}Si CP/MAS NMR. The ^{29}Si NMR results also show that the chain density on the surface increases as the percentage of short chains increases, with the single phase surface of 100% short chains having the highest density. However, the mixed phase surface incorporating 16% long chain amines is more extensively cross-linked and contains fewer unreacted hydroxyls than the single phase surface with only short chain amines. Since these unreacted hydroxyls contribute to degradation in the performance of these materials with time when they are used in HPLC columns, it is important to minimize the amount of these structures on the surface [1]. Consequently, the mixed phase surface (16% long chains) is expected to have superior stability to single phase surfaces, in agreement with previous work on mixed phase surface with different ligands [1]. Interestingly, this advantage is lost when a larger number of long chain amines are incorporated in a mixed phase surface. While superior to the single phase surface containing only long chains, the mixed phase surface containing 37% long chains exhibits slightly less cross-linking and slightly more unreacted hydroxyls than the single phase surface containing only short chains. These results suggest there is an optimum ratio for the two types of ligands in a mixed phase surface, most likely dictated by steric factors.

By contrast to ^{29}Si CP/MAS spectra, relative intensities observed in a single ^{13}C CP/MAS spectrum can be quite misleading due to differences in mobility and cross-polarization efficiency for different carbons in the chain. Accurate ^{13}C quantitative results can only be obtained by acquiring a series of spectra at different contact times and fitting these intensities as a function of contact time to obtain undistorted relative intensities. Our results demonstrate that this method can still be employed to obtain accurate quantitative results even in the case of severe spectral overlap.

The amount of long and short chains on the surface of the two mixed phase samples determined from quantitative ^{13}C NMR agrees well with that calculated from the percentages of carbon and nitrogen in the sample determined from elemental analysis. These results demonstrate that ^{13}C CP/MAS NMR can be used to determine the composition of mixed phase samples in cases where the composition cannot be determined by elemental analysis, e.g. for ligands that do not contain nitrogen. For both mixed phase samples, the actual incorporation of long chains on the surface is significantly less than the amount of long chains present in the reaction mixture. This suggests that the long chain amines are kinetically slower to react with the surface than the short chain amines, most likely due to steric hindrance. Although detailed interpretation is precluded by spectral overlap, relaxation time measurements suggest that, on mixed phase surfaces, the long chains tend to be surrounded by short chains; there is no evidence for blocks of long chains on the surface.

Acknowledgements

We are grateful to the University of Delaware for use of the Bruker MSL 300 solid-state NMR spectrometer used for this work. Separation Methods technology, Incorporated acknowledges NSF SBIR Grant # DM-9660590.

References

[1] H.O. Fatunmbi, M.D. Bruch, M.J. Wirth, Anal. Chem. 65 (1993) 2048.
[2] M. Pursch, L.C. Sander, K. Albert, Anal. Chem. 68 (1996) 4107.
[3] L. Li, P.W. Carr, J.F. Evans, J. Chromatogr. A 868 (2000) 153.
[4] K. Albert, R. Brindle, J. Schmid, B. Buszewski, E. Bayer, Chromatographia 38 (1994) 283.
[5] K. Albert, R. Brindle, P. Martin, I.D. Wilson, J. Chromatogr. A 665 (1994) 253.
[6] G.E. Maciel, C.E. Bronnimann, R.C. Zeigler, I-S. Chuang, D.R. Kinney, E.A. Keiter, Adv. Chem. Ser. 234 (1994) 269.
[7] A.B. Scholten, J.W. de Haan, H.A. Claessens, L.J.M. van de Ven, C.A. Cramers, J. Chromatogr. A 688 (1994) 25.
[8] D. Derouet, S. Forgeard, J-C. Brosse, J. Emery, J-Y. Buzare, J. Polym. Sci., Part A: Polym. Chem. 36 (1998) 437.
[9] M. Pursch, L.C. Sander, K. Albert, Anal. Chem. 71 (1999) 733A.
[10] M.J. Wirth, R.W.P. Fairbank, H.O. Fatunmbi, Science 275 (1997) 44.
[11] S.O. Akapo, H.O. Fatunmbi, LC–GC 17 (1999) 334.
[12] M. Huang, E. Dubrovcakova, M. Novotny, H.O. Fatunmbi, M.J. Wirth, J. Microcolumn Sep. 6 (1994) 571.
[13] I.S. Zagon, W.J. Hurst, P. J McLaughlin, Life Sci. 61 (1997) 1261.
[14] M. Pursch, S. Strohschein, H. Händel, K. Albert, Anal. Chem. 68 (1996) 386.
[15] M. Pursch, R. Brindle, A. Ellwanger, L.C. Sander, C.M. Bell, H. Händel, K. Albert, Solid State Nuc. Mag. Res. 9 (1997) 191.
[16] K. Albert, T. Lacker, M. Raitza, M. Pursch, H.J. Egelhaaf, D. Oelkrug, Angew Chem., Int. Engl. 37 (1998) 777.

[17] M. Pursch, L.C. Sander, H.J. Egelhaaf, M. Raitza, S.A. Wise, D. Oelkrug, J. Am. Chem. Soc. 121 (1999) 3201.
[18] M.J. Wirth, H.O. Fatunmbi, Anal. Chem. 65 (1993) 822.
[19] M.J. Wirth, H.O. Fatunmbi, Anal. Chem. 64 (1992) 2783.
[20] L.W. Jelinski, M.T. Melchior, in: M.D. Bruch (Ed.), NMR Spectroscopy Techniques, second ed., Marcel Dekker, NY, 1996.
[21] J.H. Noggle, Practical Curve Fitting and Data Analysis, Prentice Hall, NY, 1993.
[22] G.E. Maciel, D.W. Sindorf, J. Am. Chem. Soc. 102 (1980) 7607.
[23] B. Pfleiderer, K. Albert, E. Bayer, J. Chromatogr. 506 (1990) 343.
[24] K. Albert, B. Pfleiderer, E. Bayer, Chem. Modified Surf. 2 (1988) 287.
[25] R.C. Ziegler, G.E. Maciel, Chem. Modified Surf. 2 (1988) 319.
[26] K. Albert, J. Schmid, B. Pfleiderer, E. Bayer, Chem. Modified Surf. 4 (1992) 105.
[27] H.J. Egelhaaf, D. Oelkrug, A. Ellwnger, K. Albert, J. High Resol. Chromatogr. 21 (1998) 11.